This is an open access article published under a Creative Commons Attribution (CC-BY) License, which permits unrestricted use, distribution and reproduction in any medium, provided the author and source are cited.

ACS OMEGA

Article

http://pubs.acs.org/journal/acsodf

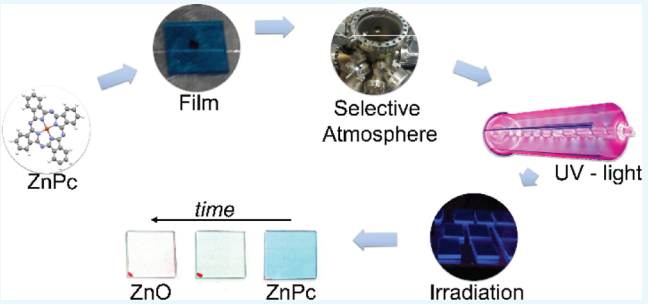
Room-Temperature Routes Toward the Creation of Zinc Oxide Films from Molecular Precursors

D. Leonardo Gonzalez Arellano,[†,§] Jasvir Bhamrah,[†] Junwei Yang,[†,∥] James B. Gilchrist,[†] David W. McComb,[‡] Mary P. Ryan,[†] and Sandrine Heutz*[,†]

[†]Department of Materials and London Centre for Nanotechnology, Imperial College London, SW7 2AZ London, U.K.

[‡]Department of Materials Science and Engineering, The Ohio State University, Columbus, Ohio 43212, United States

ABSTRACT: The fabrication of "flexible" electronics on plastic substrates with low melting points requires the development of thin-film deposition techniques that operate at low temperatures. This is easily achieved with vacuum- or solution-processed molecular or polymeric semiconductors, but oxide materials remain a significant challenge. Here, we show that zinc oxide (ZnO) can be prepared using only room-temperature processes, with the molecular thin-film precursor zinc phthalocyanine (ZnPc), followed by UV-light treatment in vacuum to elicit degradation of the organic components and transformation of the deposited film to the oxide material. The degradation mechanism was assessed by studying the influence of the atmosphere during the reaction: it was particularly sensitive to the oxygen pressure in the chamber and optimal degradation conditions were established as 3 mbar with 40% oxygen in nitrogen. The morphology of the film remained relatively unchanged during the reaction, but a detailed analysis of its composition using both scanning transmission electron microscopy and secondary ion mass spectrometry revealed that a 40 nm thick layer containing ZnO results from the 100 nm thick precursor after complete reaction. Our methodology represents a simple route for the fabrication of oxides and multilayer structures that can be easily integrated into current molecular thin-film growth setups, without the need for a high-temperature step.



INTRODUCTION

The study of transparent functional oxides has become a topic of intense research,[1] with these materials being investigated as both electrode materials and active components in optoelectronic devices. ZnO is one of the most versatile oxides, as it is a direct wide-band-gap semiconductor (3.35 eV at room temperature), which has a high exciton binding energy (60 meV), and can be doped to tune its properties. Several methods for the deposition of ZnO have been investigated, such as sol−gel,[2] molecular beam epitaxy,[3] spray pyrolysis,[4] pulsed laser deposition,[5] and electrodeposition.[6,7] One important goal of developing novel processing techniques for plastic electronics is to keep the substrate temperatures low while maintaining good electrical performance; however, a postannealing step is commonly necessary to reduce the number of defects and the accumulated strain energy[8] required to achieve a high performance, even though low-crystallinity ZnO can be achieved at lower temperatures using solution-based deposition.[9] This reduces the possibilities of using flexible substrates, such as poly(ethylene terephthalate), for next-generation electronics. Recently, new methods for postprocessing of oxide precursors deposited from solution have been used, and room-temperature photochemical treatment has been reported, although unintentional heating up to 150 °C was still observed.[10] Furthermore, deposition of metal oxides at 200 °C on hybrid organic−inorganic bilayers has been achieved using pulsed laser deposition.[11]

The search for new methods to obtain transparent conductive oxides that avoid a high thermal budget is therefore highly topical. A new method for the transformation of molecular thin films to metal oxides using UV-light treatment has been proposed by Gardener et al.[12] using two well-known molecular semiconductor materials as precursors, namely, copper and manganese phthalocyanine (CuPc and MnPc). The method relies on the degradation of the organic macrocycle of metal phthalocyanines using UV light at a wavelength of 172 nm (7.2 eV), produced from a Xe_2* excimer lamp.[13] The energy provided by the UV photons is sufficient to dissociate the most common organic bonds, such as C−C and C−N,[14] including the bond between the metallic ion and organic ring of most phthalocyanines, as reported by Liao et al.[15] The Fe, Ni, and Co central atoms in the phthalocyanines have a higher binding energy than that provided by the UV light; however, degradation of CoPc films using UV light (172 nm) has been reported,[13] which indicates that the process is not exclusively photolytic.

Received: October 19, 2016
Accepted: November 8, 2016
Published: January 12, 2017

 © 2017 American Chemical Society

DOI: 10.1021/acsomega.6b00324
ACS Omega 2017, 2, 98−104

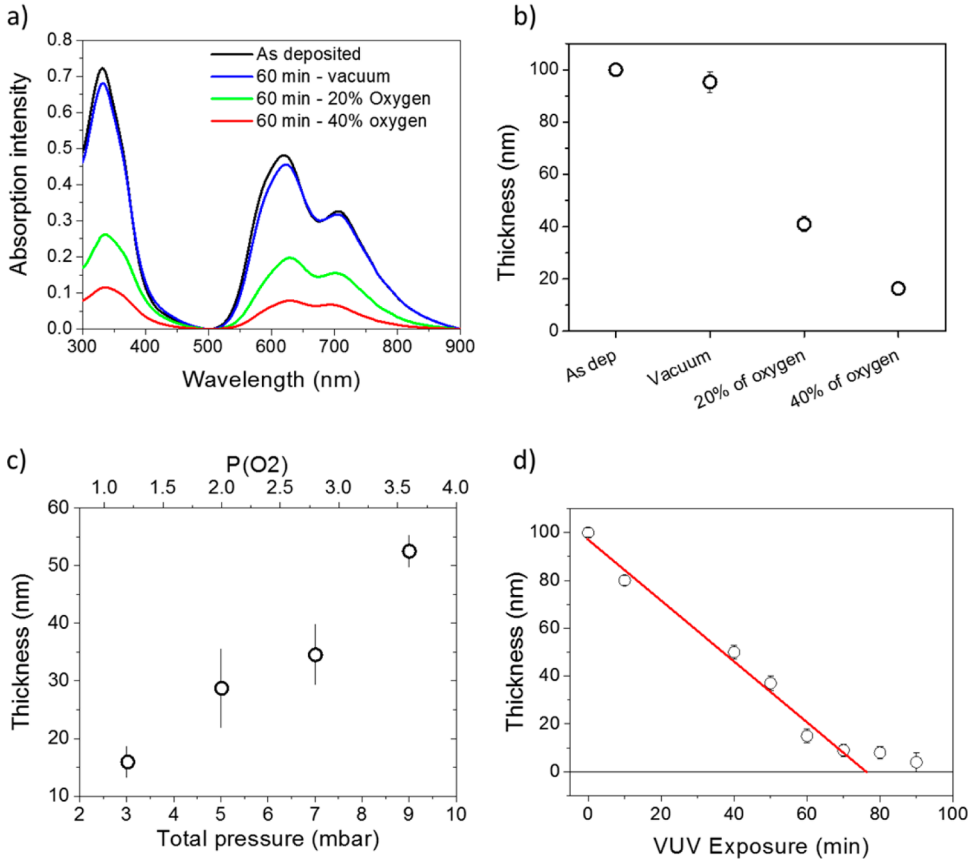


Figure 1. (a) Absorption spectra of a 100 nm ZnPc film before (black) and after 60 min exposure to UV light in vacuum (blue), and 20% oxygen partial pressure (green), and at 40% oxygen partial pressure (red). (b) Calculated residual thickness of film present before and after exposure to UV light for 60 min in vacuum and at 20 and 40% partial pressure of oxygen. (c) Estimated thickness of ZnPc films after exposure to UV light for 60 min shows the relationship between the final thickness and the total pressure in the reaction chamber. (d) Kinetics of the photodegradation process. The red line is the linear fitting of the data range, considering points between 0 and 70 min of exposure.

In this work, we explore the possibility of extending the technique to different systems, such as ZnPc, as a new alternative for low-temperature formation of ZnO. This technique offers the advantage of operating completely at room temperature, providing an easy and versatile synthesis route for the production of transparent conductive semiconductors on flexible substrates. The technique relies on the growth of molecular semiconductor thin films and only requires minimal addition to the existing setups for small-molecule-based devices, offering the prospect of significantly simplifying the fabrication of organic optoelectronic devices.

It is crucial to understand the underlying mechanism of the process and the factors that affect the degradation of the phthalocyanine films. Here, we investigate the influence of the presence of oxygen in the system, as it has proven to be a defining factor in the degradation of organic molecules,[16] mainly due to the formation of strongly oxidizing species, such as OH radicals[17] and excited oxygen species.[18,19] A standard mechanism for the full degradation of the organic film with the formation of ZnO is provided as a result of our tests under different atmospheric conditions and has been used to characterize the influence of the morphology of the starting material on the degradation of the films. We further expand the understanding of the oxide-formation process by performing elemental analysis on the treated films. Energy-dispersive X-ray (EDX) spectroscopy is used to characterize the composition of the film and to identify the position of the ZnO layer. Secondary ion mass spectrometry (SIMS) is used to quantify the amount of ZnO produced via a depth profile of the treated film and confirms that UV treatment is a viable low-temperature route for the formation of oxide-based materials from molecular semiconductor precursors.

RESULTS

To understand the role of oxygen in the degradation mechanism, the UV−vis absorption spectra of ZnPc films, with a nominal thickness of 100 nm, were recorded. Spectra from films before and after exposure to UV light for 60 min in different environments are shown in Figure 1a. The intensities of the characteristic absorption bands can be used to estimate the amount of the ZnPc film remaining, using the Beer−Lambert law. Figure 1b shows the results following integration of the Q-band region (500−800 nm, chosen because it corresponds to a relatively simple electronic transition and is free from any oxide absorption) to monitor the changes in the thickness of the molecular film.

In vacuum (10^{-5} mbar), very little degradation takes place after 60 min (Figures 1a,b). To assess the influence of the presence of oxygen, the films are exposed to a mixture of nitrogen and oxygen, with the total pressure held at 3 mbar. An oxygen concentration of 20% in the mixture results in decreased absorption, in the 500−800 nm range, due to faster degradation of the Pc ring, and a further increment in the oxygen partial pressure to 40% accelerates this degradation

DOI: 10.1021/acsomega.6b00324
ACS Omega 2017, 2, 98−104

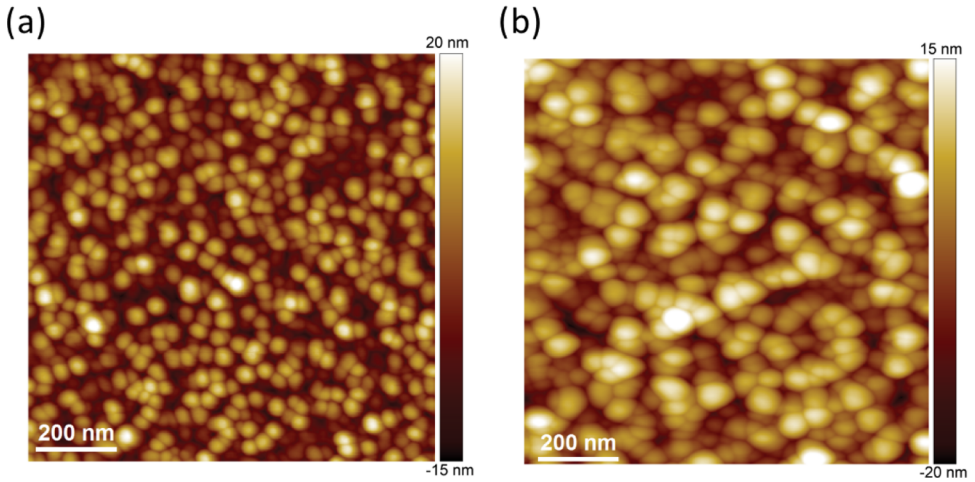


Figure 2. AFM images of a 100 nm thick ZnPc film before and after exposure to UV light under standard atmospheric conditions. (a) Untreated ZnPc film and (b) ZnPc film after irradiation for 90 min.

Table 1. Elemental Composition, Expressed in mass%, of a 100 nm ZnPc Thin Film before and after Exposure to UV Light Obtained by EDX[a]

	C	N	O	Zn	C/Zn (32)	C/N (4)	N/Zn (8)	O/ Zn
0 min	82.9 ± 0.6	13.8 ± 0.9	2.1 ± 0.5	1.1 ± 0.2	73.4	6.0	12.2	2.0
90 min	79.4 ± 0.4	8.4 ± 0.3	9.9 ± 0.3	2.3 ± 0.1	34.5	9.4	3.7	5.0

[a]The error corresponds to the standard deviation from multiple measurements.

process (Figure 1a,b). The results obtained indicate that the presence of oxygen increases the speed of the reaction; such a behavior was previously observed for UV exposure of self-assembled monolayers.[16] The dependence on oxygen can be due to the formation of strong reactants, such as OH radicals and excited oxygen molecules, resulting in the generation of ozone and oxygen radicals in the singlet (O(1D)) and triplet (O(3P)) states on interaction with UV light, as expressed in eq 1[17,18]

$$O_2 + h\nu \rightarrow O(1D) + O(3P) \quad (\lambda \leq 172\ \text{nm}) \qquad (1)$$

A further increase in oxygen pressure produces a deceleration of the degradation rate. This is shown by increasing the total pressure from the vacuum condition in the reaction chamber, keeping the partial pressure of oxygen at 40%. The equivalent thickness of ZnPc remaining after treatment for 60 min is shown in Figure 1c. The deceleration in degradation could be a direct result of the attenuation of UV light by molecular oxygen (the absorption cross section is 6×10^{-19} cm^2 at 172 nm).[22] At a partial pressure of oxygen of 0.2 mbar, the attenuation of UV light before reaching the film is 7%; it is 13% at 1.2 mbar and rises to 31% at 3 mbar. From these results, we can conclude that a combination of 1.2 mbar of oxygen with 1.8 mbar of nitrogen (i.e., 40% partial pressure of oxygen at 3 mbar) is the most effective environment for the degradation of ZnPc films and will be used as the standard condition henceforth.

A second parameter influencing the degradation of the films is the total photon dose delivered by the UV lamp, which is directly proportional to the irradiation time for a fixed intensity of light. The degradation of a series of 100 nm thick ZnPc films as a function of the irradiation time in the standard atmosphere established earlier is presented in Figure 1d. The results show a decrease in the absorption intensity for longer irradiation times. The degradation follows a linear trend until ∼70 min of irradiation, indicating a first-order rate law, with a time constant of 1.2 nm/min. Following degradation of 95 nm ZnPc at ∼70 min, the degradation slows and a plateau is reached. This could be due to the higher error in estimating low thicknesses or is more likely an indication of the formation of a surface layer blocking further degradation of ZnPc at the substrate interface.

The morphology of the material was studied by atomic force microscopy (AFM). The untreated 100 nm thick ZnPc film shown in Figure 2a is uniformly covered with spherical grains, with diameters of approximately 40 nm, and leading to a root-mean-square (RMS) surface roughness of 6 nm.

Figure 2b shows a 100 nm ZnPc film after irradiation with UV light under standard conditions for 90 min. The RMS roughness of the treated film is 6 nm, the spherical shape of the grains is maintained, and the overall diameter of the grains increases to approximately 50 nm; however, smaller grains can also be observed. The conservation of the morphology in fully degraded Pc films is in agreement with previous work on other metal Pc's.[13,14]

The results of the EDX analysis of the films in top view (i.e., through the different layers of the film and excluding Pt and Cr contributions) are presented in Table 1.

Although absolute values of composition should be treated with caution due to the contribution of the grid, residual oxygen (e.g., showing a contribution on the pristine film), and the errors associated with using the Cliff–Lorimer approach, clear trends can be identified. The decrease in the C/Zn and N/Zn ratios indicates the loss of organic material, in agreement with the spectroscopic observations. Conversely, the relative quantity of O measured after irradiation increases and the O/Zn ratio more than doubles compared to that for the fresh film. This is in line with the potential formation of a layer containing ZnO, although organic fragments are likely to remain.

Insight into the final thickness and composition of the degraded films can be gathered from cross-sectional scanning transmission electron microscopy (STEM) imaging and SIMS

DOI: 10.1021/acsomega.6b00324
ACS Omega 2017, 2, 98−104

studies. The top left panel in Figure 3a shows an STEM image of a cross section taken from a ZnPc film after exposure to UV

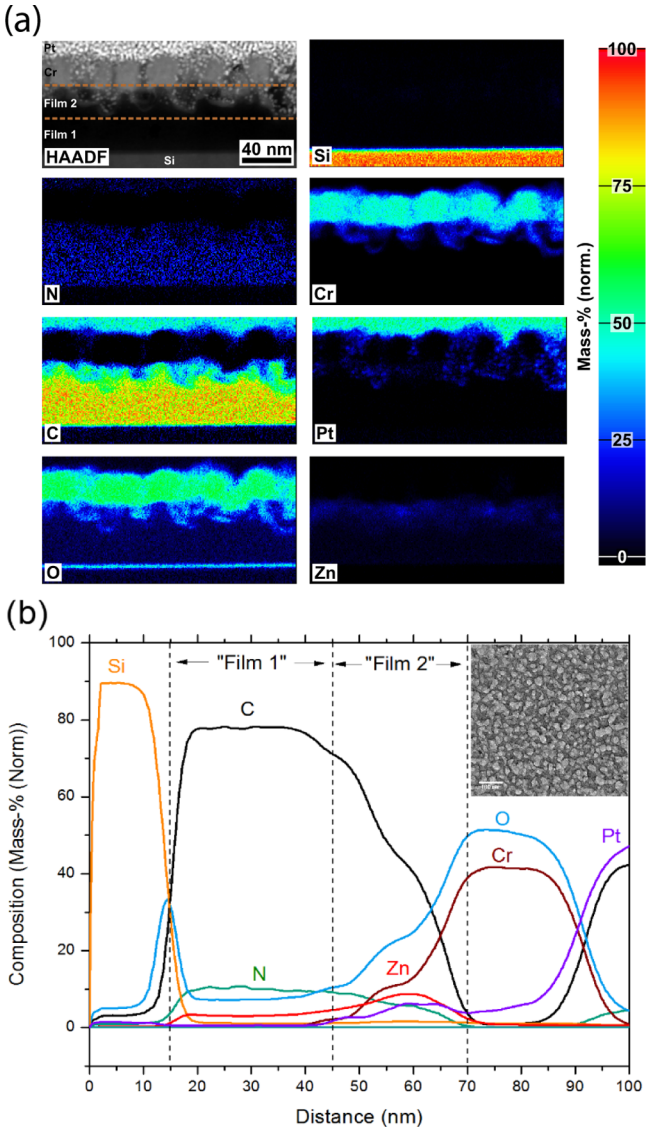


Figure 3. (a) HAADF image of a cross section of a 100 nm ZnPc film after exposure to UV light for 90 min under standard atmospheric conditions, and elemental maps of the constituent elements and coating layers of the cross section obtained by EDX. (b) Line profile of the full width of the element maps in (a); inset shows a top-view TEM image of a treated film, the scale in the inset is 100 nm.

light for 90 min. This has been acquired using a high-angle annular dark field (HAADF) detector. When imaging using HAADF STEM, the image intensity is roughly proportional to the square of the atomic number in the sample, that is, regions composed of a higher number of Z elements appear brighter.[23] Several regions characteristic of the film can be identified on the basis of contrast. A low Z and a homogeneous "film 1" region of thickness 30−40 nm appears directly above the Si substrate. The "film 2" region contains a mixture of Cr coating (originating from TEM sample preparation) and low-density material and has a thickness of 20−30 nm.

The remaining panels in Figure 3a show quantitative (mass %) EDX maps obtained from the treated sample. We have previously shown that this technique is able to accurately reflect the composition of molecular layers, including that of complex bilayer structures.[21] We can identify a C-rich layer originating at the Si interface, with a thickness of 60 nm, which also shows a weak signal from N, suggesting the possibility of the presence of ZnPc film residues after UV treatment. Cr and Pt are found on top of the region labeled film 2. The presence of Cr in film 2 is consistent with its diffusion through the deep troughs created by irradiation of the film, as seen in AFM (Figure 2b). The O map reveals that most of the oxygen content is located at the Cr coating and the SiO_2 interface; however, some O can be distinguished at the interface with film 2, and it is also at this interface that we find the highest concentration of Zn.

The maps were used to extract compositional line profiles from the quantified data, shown in Figure 3b. We observe that 80% of the region labeled film 1 is composed of C, and within the same region, N counts reach 10%. The film 2 region shows a decrease in both the C and N counts and an increase in the Zn and O counts, giving a O/Zn ratio of approximately 3. The existence of a Cr signal in this region is attributed to the diffusion of Cr particles through the less dense areas of the film, as the film is found to have a number of pinholes, as shown in the top-view TEM image (inset).

Figure 4 illustrates a depth profile analysis performed on the ZnPc films before and after irradiation using SIMS. In the as-deposited film, the C^+ and Zn^+ signals are stable after an approximate depth of 5 nm, corresponding to the transient region. The interface with silicon is identified as the point at which there is a distinct decrease in the intensity of Zn^+, C^+, and N^+ ions due to collision cascade-induced mixing, resulting in an accumulation of these ions on encountering the higher-density substrate,[24] and this is indicated by a dashed line. As the thickness of the film has been confirmed to be 100 nm, this gives a sputter rate of the as-deposited ZnPc of ∼0.47 nm s^{-1}. It is important to note that ZnO fragments are produced following interaction of ZnPc with the O_2^+ primary beam in SIMS, but their intensity is below 10 counts and can be considered negligible.

As the relative yields of the fragments depend on the precise parameters of the SIMS experiments, we use a 50 nm thick ZnO film prepared using pulsed laser deposition as a reference material[25] to be able to quantify the amount of ZnO produced by the irradiation process. The SIMS profile of the reference film in Figure 4b shows a steady number of counts of Zn^+ and ZnO^+, with a negligible value of C^+ counts, as expected.

The SIMS profile of the ZnPc film subjected to UV treatment for 90 min under standard atmospheric conditions, in Figure 4c, reveals that the C^+ signal is approximately 1 order of magnitude lower at the beginning of the measurement compared to that for the as-deposited film (see Figure 4a). C^+ decreases monotonically as a function of depth, indicating the presence of carbon-rich material on the substrate surface. The Si^+ signal is recorded from the start of the measurement, an observation attributed to the existence of pinholes in the treated sample.

The Zn^+ signal intensity is 1 order of magnitude higher than that for the starting film, with values similar to those observed in a reference ZnO sample (Figure 4c), suggesting that some of the ZnPc has been transformed into ZnO. The slightly higher counts as compared to the reference value can be attributed to a matrix effect generated by the mixture of the residual film and ZnO and the uncertainty in the sputtering rate in this complex material. The degree of ZnO formation after UV treatment of the ZnPc film can therefore be more reliably assessed by

DOI: 10.1021/acsomega.6b00324
ACS Omega 2017, 2, 98−104

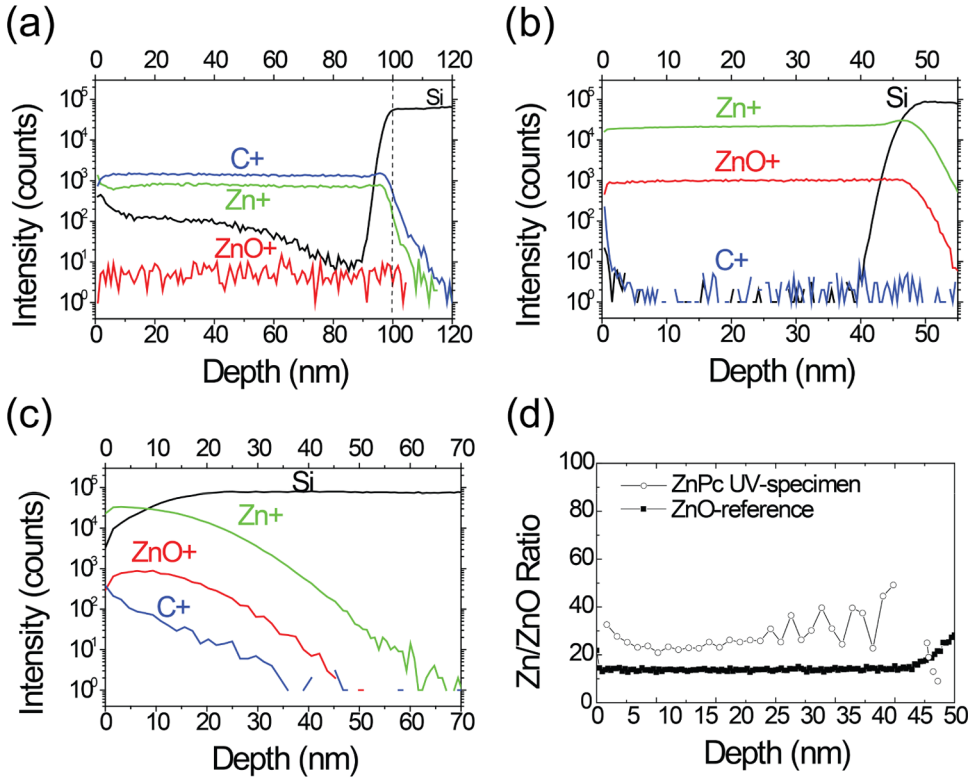


Figure 4. SIMS depth profile of a 100 nm ZnPc film deposited on Si. (a) ZnPc film as-deposited. (b) 50 nm ZnO as-deposited. (c) ZnPc film after 90 min of exposure to UV under standard conditions. (d) Ratio of Zn^+/ZnO^+ in the treated sample (open circles) and the ZnO^+ reference (solid squares). The dashed line indicates the interface between the film and Si substrate.

comparing the ratio, $R = [Zn^+]/[ZnO^+]$, from the reference and treated film, as shown in Figure 4d. The higher ratio in the UV-treated sample compared to that for ZnO indicates that a fraction of the Zn^+ signal originates from the ZnPc fragments, in line with the UV−vis results in Figure 1, which showed evidence of residual ZnPc even after prolonged UV exposure. This fraction can be quantified using eq 2, in which the subscripts UV, ref, and ZnPc refer to the ratios obtained in the degraded sample, the ZnO reference, and the ZnPc film, respectively.

$$R_{UV} = xR_{ref} + (1 - x)R_{ZnPc} \quad (2)$$

Solving for "x", the percentage of Zn^+ that is generated from the ZnO obtained is approximately 85−90%.

This result allows us to unambiguously prove that UV treatment of ZnPc can lead to the dissociation of the organic ring and promote the formation of ZnO.

CONCLUSIONS

We have developed a versatile new method for producing ZnO from a ZnPc precursor at low temperatures using an excimer, UV light, to promote the degradation of the organic macrocycle. The exposure of a film of ZnPc with a starting thickness of 100 nm for 90 min to a mixture of oxygen and nitrogen results in near-complete degradation of the phthalocyanine film, as can be derived by its transparency in the visible range. By controlling the partial pressure of oxygen in the reaction chamber, we were able to show that the efficiency of degradation is mediated by oxygen but excess oxygen is detrimental due to significant absorption of the UV light reaching the surface of the film. Cross-sectional HAADF−TEM imaging shows that the morphology is inhomogeneous through the thickness of the film, with the top surface enriched in Zn and O. A more quantitative analysis is performed using time-of-flight (TOF)-SIMS, which highlights that a layer containing 85−90% of ZnO is formed, and the remaining material is composed of residual organic fragments from the degradation process. Our results offer a route for the creation of metal oxides entirely at low temperatures, using precursor materials and processes that are already of widespread use in the field of organic electronics. This methodology therefore not only represents a significant reduction of the thermal budget in the fabrication of functional oxide materials but also opens up unique perspectives, for example, in the creation of hybrid structures.

EXPERIMENTAL SECTION

For the preparation of the substrates, glass, quartz, and Si (100) were cleaned in acetone and isopropyl alcohol using an ultrasonic bath for 10 min and then dried with nitrogen and immediately put inside the evaporation chamber. For TEM imaging in top view, Nickel (3.05 mm diameter, 150 square mesh grids) and a continuous carbon film are used (Agar). ZnPc (Aldrich, 97%) thin films were grown to a nominal thickness of 100 nm at a base pressure of 10^{-7} mbar using a SPECTROS organic molecular beam deposition chamber (Kurt J. Lesker). During the deposition process, the substrates were kept at room temperature and the source Knudsen cell was heated to a maximum temperature of 420 °C; the deposition rate was 1 Å/s, monitored using a quartz crystal microbalance.

UV treatment of the specimens was performed in a purpose-built vacuum chamber using a UV lamp source from Hereaus (BlueLight compact 172/120 Z), with a nominal irradiance of 50 mW/cm^2 and the sample located at a distance of 7 cm from

DOI: 10.1021/acsomega.6b00324
ACS Omega 2017, 2, 98−104

the UV source, with the film facing toward the UV lamp during irradiation. To obtain a controlled atmosphere during treatment, the system pressure was brought to 10^{-2} mbar using a rotary pump and filled with N_2 (99.998%) and O_2 (99.5%) gases (BOC gases Ltd) to the stoichiometry and pressure values specified in the text using a MKS 1179A mass flow controller. For experiments in vacuum, the chamber was pumped down to 10^{-5} mbar using a turbomolecular pump. Following stabilization of the pressure, the UV lamp was powered on for the desired period of time. The system pressure was then lowered back to 10^{-2} mbar for 5 min to remove residual gases and then vented. During the entire irradiation process the maximum temperature of the substrate was monitored and maintained below 80 °C, typically at room temperature. The samples were stored in a desiccator until use.

Electronic (UV−visible) absorption characterization was carried out using a Perkin-Elmer Lambda 25 UV/vis spectrophotometer, with a slit width of 1 mm. AFM measurements were obtained with a Veeco Dimension 3100 AFM in the tapping mode, using a Si probe from MikroMasch, with a drive frequency close to 300 kHz. The top-view TEM image and corresponding EDX in Table 1 were obtained on a JEOL 2010 TEM operated at 200 kV; the specimen was imaged at 0° tilt and with the objective aperture inserted. The EDX detector was an Oxford Instruments INCA EDX 80 mm X-Max detector system. The elemental composition was obtained using the INCA software, considering the Kα lines from C, N, O, and Zn and deriving the mass % from theoretical Cliff−Lorimer *k*-factors. Cross-sections were prepared using an FEI Helios Nanolab 600 dual-beam instrument, where a scanning electron microscope is combined with a Ga^+ focused ion beam. Final thinning was performed at 1 keV and 3.2 pA.[20,21] To prevent significant beam-induced damage to surface features, the organic films were coated with Cr before being exposed to either the electron or ion beam. Pt was deposited in situ to add further protection. The EDX composition maps on the cross-sections were obtained on an FEI Tecnai Osiris STEM, operated at 200 kV with a windowless Super-X SDD array. Postprocessing was performed using Esprit 1.9 from Bruker. SIMS analysis was performed on a TOF-SIMS[5] by IONTOF. The primary ion beam used was 1 keV O_2^+ at 170−200 nA over an area of 450 × 450 μm^2, and the analytical beam used was 25 keV $Bi^{3,+}$ with a current of 0.53 pA over an area of 100 × 100 μm^2. Both beams have incidence angles of 45°, and the base pressure of the chamber during the measurements was 1.6 × 10^{-8} mbar.

AUTHOR INFORMATION

Corresponding Author

*E-mail: s.heutz@imperial.ac.uk.

Present Addresses

[§]Department of Polymer Science and Engineering, University of Massachusetts, Amherst, Massachusetts 01003, United States (D.L.G.A.).

[∥]Department of Engineering, University of Cambridge, CB3 0FA Cambridge, U.K. (J.Y.).

Author Contributions

The manuscript was written through contributions from all authors. All authors have given approval to the final version.

Notes

The authors declare no competing financial interest.

ACKNOWLEDGMENTS

We thank the National Council for Science and Technology (CONACyT) for financial support. We also thank Dr. Sarah Fearn for help and guidance with SIMS measurements and Drs. Luke Fleet and Mahmoud Ardakani for useful discussions.

REFERENCES

(1) Facchetti, A.; Marks, T. *Transparent Electronics: From Synthesis to Applications*; Wiley-Blackwell: Chippenham, 2010, pp 1−470.

(2) Yang, T.; Cai, W.; Qin, D.; Wang, E.; Lan, L.; Gong, X.; Peng, J.; Cao, Y. Solution-Processed Zinc Oxide Thin Film as a Buffer Layer for Polymer Solar Cells with an Inverted Device Structure. *J. Phys. Chem. C* **2010**, *114*, 6849−6853.

(3) Fujita, M.; Kawamoto, N.; Sasajima, M.; Horikoshi, Y. Molecular Beam Epitaxy Growth of ZnO Using Initial Zn Layer and MgO Buffer Layer on Si(111) Substrates. *J. Vac. Sci. Technol., B* **2004**, *22*, 1484−1486.

(4) Peiro, A. M.; Ravirajan, P.; Govender, K.; Boyle, D. S.; O'Brien, P.; Bradley, D. D. C.; Nelson, J.; Durrant, J. R. Hybrid Polymer/Metal Oxide Solar Cells Based on ZnO Columnar Structures. *J. Mater. Chem.* **2006**, *16*, 2088−2096.

(5) Choopun, S.; Vispute, R. D.; Noch, W.; Balsamo, A.; Sharma, R. P.; Venkatesan, T.; Iliadis, A.; Look, D. C. Oxygen Pressure-Tuned Epitaxy and Optoelectronic Properties of Laser-Deposited ZnO films on Sapphire. *Appl. Phys. Lett.* **1999**, *75*, 3947−3949.

(6) Peulon, S.; Lincot, D. Cathodic Electrodeposition from Aqueous Solution of Dense or Open-Structured Zinc Oxide Films. *Adv. Mater.* **1996**, *8*, 166−170.

(7) Cruickshank, A. C.; Tay, S. E. R.; Illy, B. N.; Da Campo, R.; Schumann, S.; Jones, T. S.; Heutz, S.; McLachlan, M. A.; McComb, D. W.; Riley, D. J.; Ryan, M. P. Electrodeposition of ZnO Nanostructures on Molecular Thin Films. *Chem. Mater.* **2011**, *23*, 3863−3870.

(8) Zhu, B. L.; Zhao, X. Z.; Su, F. H.; Li, G. H.; Wu, X. G.; Wu, J.; Wu, R. Low Temperature Annealing Effects on the Structure and Optical Properties of ZnO Films Grown by Pulsed Laser Deposition. *Vacuum* **2010**, *84*, 1280−1286.

(9) Meyers, S. T.; Anderson, J. T.; Hung, C. M.; Thompson, J.; Wager, J. F.; Keszler, D. A. Aqueous Inorganic Inks for Low-Temperature Fabrication of ZnO TFTs. *J. Am. Chem. Soc.* **2008**, *130*, 17603−17609.

(10) Kim, Y.-H.; Heo, J.-S.; Kim, T.-H.; Park, S.; Yoon, M.-H.; Kim, J.; Oh, M. S.; Yi, G.-R.; Noh, Y.-Y.; Park, S. K. Flexible Metal-Oxide Devices Made by Room-Temperature Photochemical Activation of Sol-Gel Films. *Nature* **2012**, *489*, 128−132.

(11) Franklin, J. B.; Downing, J. M.; Giuliani, F.; Ryan, M. P.; McLachlan, M. A. Building on Soft Foundations: New Possibilities for Controlling Hybrid Photovoltaic Architectures. *Adv. Energy Mater.* **2012**, *2*, 528−531.

(12) Gardener, J. A.; Liaw, I.; Aeppli, G.; Boyd, I. W.; Fiddy, S.; Hyett, G.; Jones, T. S.; Lauzurica, S.; Palgrave, R. G.; Parkin, I. P.; Sankar, G.; Sikora, M.; Stoneham, A. M.; Thornton, G.; Heutz, S. Oxide Nanoparticle Thin Films Created Using Molecular Templates. *J. Phys. Chem. C* **2011**, *115*, 13151−13157.

(13) Ohta, N.; Gomi, M. Photochemical Decomposition of Co Phthalocyanine Films Using Ultraviolet Excimer Lamp. *Jpn. J. Appl. Phys., Part 1* **2000**, *39*, 4195−4197.

(14) Gardener, J. *Molecular Thin Films: Fundamentals and Potential Routes for Spintronic Applications*; University College London: London, 2008; pp 1−246.

(15) Liao, M.-S.; Scheiner, S. Electronic Structure and Bonding in Metal Phthalocyanines, Metal = Fe, Co, Ni, Cu, Zn, Mg. *J. Chem. Phys.* **2001**, *114*, 9780−9791.

(16) Sugimura, H.; Hong, L.; Lee, K. H. Photochemical Oxidation of Chloromethylphenylsiloxane Self-Assembled Monolayer Amplified with Atmospheric Oxygen and its Application to Micropatterning. *Jpn. J. Appl. Phys., Part 1* **2005**, *44*, 5185−5187.

(17) Roland, R. P.; Bolle, M.; Anderson, R. W. Low Temperature Photochemical Vapor Deposition of SiO_2 Using 172 nm Xe_2* Excimer

DOI: 10.1021/acsomega.6b00324
ACS Omega 2017, 2, 98−104

Lamp Radiation with Three Oxidant Chemistries: O^{-2}, H_2O/O^{-2}, and H_2O_2. *Chem. Mater.* **2001**, *13*, 2493−2500.
(18) Saito, N.; Hayashi, K.; Sugimura, H.; Takai, O. The Decomposition Mechanism of p-chloromethylphenyltrimethoxysiloxane Self-Assembled Monolayers on Vacuum Ultraviolet Irradiation. *J. Mater. Chem.* **2002**, *12*, 2684−2687.
(19) Chao, S. C.; Pitchai, R.; Lee, Y. H. Enhancement in Thermal Oxidation of Silicon by Ozone. *J. Electrochem. Soc.* **1989**, *136*, 2751−2752.
(20) Lekstrom, M.; McLachlan, M. A.; Husain, S.; McComb, D. W.; Shollock, B. A. Using the *In Situ* Lift-Out Technique to Prepare TEM Specimens on a Single-Beam FIB Instrument. *J. Phys.: Conf. Ser.* **2008**, *126*, No. 012028.
(21) Gilchrist, J. B.; Basey-Fisher, T. H.; Chang, S. C.; Scheltens, F.; McComb, D. W.; Heutz, S. Uncovering Buried Structure and Interfaces in Molecular Photovoltaics. *Adv. Funct. Mater.* **2014**, *24*, 6473−6483.
(22) Eliasson, B.; Kogelschatz, U. UV Excimer Radiation from Dielectric-Barrier Discharges. *Appl. Phys. B* **1988**, *46*, 299−303.
(23) Williams, D. B.; Carter, C. B. *Transmission Electron Microscopy: A Textbook for Materials Science*; Springer US: New York, 2009; pp 369−578.
(24) Vickerman, J. C. *Surface Analysis: The Principal Techniques*; Wiley: Chichester, 1997; pp 113−268.
(25) Franklin, J. B.; Zou, B.; Petrov, P.; McComb, D. W.; Ryan, M. P.; McLachlan, M. A. Optimised Pulsed Laser Deposition of ZnO Thin Films on Transparent Conducting Substrates. *J. Mater. Chem.* **2011**, *21*, 8178−8182.

DOI: 10.1021/acsomega.6b00324
ACS Omega 2017, 2, 98−104